Synthesis of KOH-activated carbon aerogel for the efficient removal of crystal violet from aqueous solutions

Nguyen Thi Hai Yen*, Tran Anh Khoi, Nguyen Van Dung
Institute for Tropicalization and Environment.
*Corresponding author: yen.nth98.chem@gmail.com
Received 01 Nov 2022; Revised 21 Nov 2022; Accepted 14 Dec 2022; Published 20 Dec 2022.
DOI: https://doi.org/10.54939/1859-1043.j.mst.VITTEP.2022.51-61

ABSTRACT

In this study, a low-cost jackfruit based KOH-activated carbon aerogel (AJCA) is prepared from facile hydrothermal treatment synthesized core of jackfruit with different heating rate. AJCA is sythesisized to absorb crystal violet (CV) dye from aqueous solutions and effectively treat other dyes. Scanning electron microscopy (SEM) and energy dispersive X-ray spectroscopy (EDS) allow for targeted analysis of sample surfaces which has many grooves of varying depth, and many layers of scales stack on top of each other. The specific surface area, which is examined by The Brunauer-Emmett-Teller (BET) method, reaches 592.65 m^2/g. The most suitable heating rate is 3 degrees per minute (AJCA-3). The maximum adsorption capacity is 386,66 mg/g and the absorption performance reaches 96,5% at a concentration of 300 ppm, which indicates that AJCA-3 is very efficient and competitive with several adsorbents. The pseudo-second-order model satisfactorily describes the adsorption kinetics, and the Langmuir model was suitable to represent the adsorption equilibrium. These experiments show that AJCA has excellent potential on treating real coloured effluents.

Keywords: Activated carbon aerogel; Efficent; Crystal violet.

1. INTRODUCTION

In recent years, the rapid development of industry leads to a large amount of water pollution [1]. It is estimated that more than 700,000 types of dyestuffs which are annually emitted from various industries such as textile, paper, cosmetics, food, etc. into the aquatic environment [2]. In the year 2050, without appropriate and strong policies to manage water resources, increased water demand can deplete groundwater resources, and eutrophication, affecting aquatic biodiversity and human life [3].

Synthetic dyes are mostly organic compounds with complex molecular structures, high stability [4]. Crystal Violet (CV), a triphenylmethane dye, causes serious water pollution problems, directly affects aquatic ecosystems and human life. CV interferes with photosynthetic activities at low concentrations; In several cases, CV can cause human's permanent blindness, and kidney and respiratory problems [5]. However, CV is still widely used in industrial sectors, mainly the textile industry. Therefore, it is very important to remove CV from water sources.

Electrochemical treatment techniques, chemical oxidation, ozonation, nanofiltration, and reverse osmosis, etc. are studied to treat water containing CV [6]. The biological treatment effectively removes dyes but not watercolors due to their high stability and resistance to microbial degradation [7]. Oxidation is the most commonly used chemical process for dye degradation due to its ease of use and the ability to degrade molecules. However, this process can form sludge [8]. Among the physical methods, adsorption is the most popular and cost-effective method, so it is widely applied to large scale [2].

The trend of making carbon materials of agricultural origin for water treatment adsorption is more interesting than traditional adsorbent materials with many advantages such as high efficiency, cost savings, and degradability [9]. The carbon material is synthesized by pyrolysis aerogel to create an aerogel that retains the natural structure of the base material. Carbon aerogel

can be produced in a green process, using fewer chemicals, cheaper, and more durable than hydrocarbon precursors. Converting agricultural by-products into valuable products will not only improve the economy but also reduce environmental pollution [10].

Carbon aerogel from jackfruit was reported to have a high specific surface area at 512.42 m^2/g and high stability, making it suitable as an adsorbent, electrode and supercapacitor with high specific capacitance reaching 323.8 F/g [10-12]. According to the authors' research, there have been no studies on carbonizing aerogel from jackfruit's core for gas adsorption. In this study, carbon aerogel from jackfruit core was synthesized to enhance the adsorption capacity for CV.

2. MATERIALS AND METHODS

2.1. Theoretical foundations

2.1.1. Model of adsorption isotherm

The adsorption isotherm represents the relationship between the amount of adsorbent per unit mass of the adsorbent at constant temperature and the concentration in the solution at equilibrium. Several isothermal models have been used to evaluate the adsorption equilibrium such as Langmuir, Freundlich, Redlich Peterson, Dubinin-Radushkevich, Sips, and Temkin [13]. Among them, Langmuir and Freundlich isotherm models are most commonly used.

The Langmuir adsorption isotherm model, the adsorption takes place simultaneously at different sites in the adsorbent and the adsorption is monolayer, the maximum adsorption occurs when the adsorbed molecules form a single - saturated layer on the surface of the adsorbent [14]. In a liquid-solid system, the Langmuir isotherm is described in equation (1):

$$q_e = \frac{Q_m b C_e}{1+bC_e} [15] \quad (1)$$

Where: q_e: Adsorption capacity at the time of equilibration, mg/g.

C_e: Solution concentration at the time of equilibrium, mg/L.

Q_m: Maximum adsorption capacity of the adsorbent, mg/g.

b: Langmuir adsorption constant, L/mg.

It is possible to return the Langmuir equation to a linear form if equation (1) is inverse:

$$\frac{C_e}{q_e} = \frac{1}{Q_m} C_e + \frac{1}{Q_m * b} \quad (2)$$

The Freundlich adsorption isotherm model, it is assumed that the adsorption takes place on a heterogeneous surface. The Freundlich adsorption isotherm is expressed by equation (3):

$$q_e = K_f C_e^{1/n} [16] \quad (3)$$

Where: q_e: Adsorption capacity at the time of equilibration, mg/g.

C_e: Solution concentration at the time of equilibrium, mg/L.

K_f: Freundlich adsorption constant, mg/g.

n: Adsorption strength.

Logarithmic equation (3) we get the linear form of Freundlich's equation

$$lnq_e = lnK_f + \frac{1}{n} lnC_e \quad (4)$$

Constructing a graph of $\ln q_e$ depending on $\ln C_e$, we can determine the adsorption constant K_f and the exponent n. K_f is related to adsorption capacity and 1/n is a measure of adsorption strength or surface heterogeneity. The value of 1/n ranges from 0 to 1, the adsorption becomes more heterogeneous when the value of n is close to 0 [17].

2.1.2. Adsorption kinetics

The kinetic study is an important part of adsorption research because it explains the rate of adsorption, thereby predicting the mechanism of the process and the steps controlling the rate. The adsorption kinetics determines the retention time, thereby determining the reactor size.

The apparent first-order kinetics (pseudo-first-order) assumes that the adsorption occurs only on local sites, unrelated to the interaction between the adsorbed ions, and the energy of the adsorption is independent. Depending on the surface coverage, the maximum adsorption corresponds to a saturated adsorbent layer on the surface of the adsorbent, and the concentration of the adsorbent is assumed to be constant [18].

The equation of the first-order apparent adsorption kinetics model for the solid-liquid adsorption system is shown in equation (5):

$$\frac{dq_t}{dt} = k_1(q_e - q_t) \text{ [19]} \quad (5)$$

Where q_t, q_e : Adsorption capacity at time t and time of equilibrium, mg/g.

t: Time, min.

k_1: Speed constant, 1/min.

The boundary conditions, the linear equation (6) is established:

$$ln(q_e - q_t) = lnq_e - k_1 t \quad (6)$$

Graph $\ln(q_e - q_t)$ against t, from which k_1 and q_e can be determined.

The second-order apparent adsorption kinetics model has the same assumptions as the first-order apparent kinetics model. The apparent second-order kinetic model of adsorption takes into account the rate-limiting step when forming chemical bonds during adsorption [20]. The rate of the adsorption process depends on the adsorption capacity at time t and the time of equilibrium according to equation (7):

$$\frac{dq_t}{dt} = k_2(q_e - q_t)^2 \text{[21]} \quad (7)$$

k_2: Rate constant according to the apparent quadratic kinetic model (g/(mg.time)).

q_t, q_e: Adsorption capacity at the time of equilibrium with time t (mg/g).

Applying the boundary condition, equation (7) becomes equation (8):

$$\frac{t}{q_t} = \frac{1}{k_2 q_e^2} + \frac{t}{q_e} \quad (8)$$

Construct a graph of t/qt against t, from which we determine the values of q_e and k_2.

2.2. Experiment preparation

2.2.1. Instrumentation

Scanning electron microscope and energy dispersive X-ray spectroscopy equipment (SEM-EDS) determine surface morphology and the existence and content of elements in the composition of the sample. BET surface area analysis equipment shows the specific surface area and average capillary size. Fourier-transform infrared spectroscopy equipment (FTIR) determines the functional group and chemical structure of the sample.

CV solution was determined at a wavelength of 585 nm by using a UV-VIS spectrophotometer. In the pH experiments, the CV solution pH was adjusted from 3.0 to 11.0 with hydrochloric acid and sodium hydroxide solution. The adsorption isotherms, and kinetics were studied by analyzing 0.5 g of adsorbent in 100 mL of solution at different initial CV concentrations. At the end of the adsorption experiment, the adsorbent was separated from the solution by filtering. Then, the absorbance of the filtrate dye was measured using a spectrophotometer at a wavelength of 585 nm [22]. The residual concentration of CV dye in the

aqueous solution was calculated using the initial dye concentration and absorbance values before and after adsorption. The adsorption capacity at time t and removal rate of CV by samples were calculated using the following equation:

$$q_t = \frac{(C_0 - C_t)V}{M} \quad (9)$$

$$R = \frac{C_0 - C_t}{C_0} \times 100\% \quad (10)$$

Where q_t (mg/g) is the adsorption capacity of CV; C_0 and C_t (mg/L) are the concentrations at initial and time t, respectively; V (L) is the volume of the reaction solution; M (g) is the weight of sample; and R (%) is the removal rate of CV by sample.

2.2.2. Experimental materials

Jackfruit's core was collected from the Phu Nhuan market. All chemicals in this study are from China. After collection, Jackfruit's core was washed with deionized water to remove dust, and then cut into 3 x 3 x 3 cm^3 pieces. Then, Jackfruit's core was put into the hydrothermal pot so that the Jackfruit's core and deionized water account for 60% of the volume of the hydrothermal pot. The hydrothermal pot was placed in the drying oven and heated to 180 ^oC. The hydrothermal process was carried out for 10 h, after which the drying oven was turned off and the hydrothermal pot was naturally brought to room temperature. After the hydrothermal process, the hydrogel was formed and washed 2-3 times with a mixture of ethanol/H_2O solution (v/v = 1/1) to clean the hydrogel. The hydrogel was then frozen with liquid nitrogen and freeze-dried for 48 h to form a jackfruit aerogel (JA).

The aerogel was pyrolysis to carbon aerogel by a tubular furnace. The furnace was heated slowly at 6 °C/min and heated to temperatures up to 700 °C. The pyrolysis process was maintained for 1 h with an N_2 gas atmosphere and a gas flow rate of 100 ml/min.

Carbon aerogel was mixed with KOH according to the mass ratio KOH/CA = 5 in 50 ml of water. The mixture had been keep for 24 hours and then filter the solids. The solid was dried at 110 °C until the mass remained constant. The solid was calcined at 700 ^oC for 1 hour at a heating rate of 3, 6, and 9 ^oC/min. After the activation process, the solid was cooled down and washed with deionized water to pH = 7 to obtain the samples AJCA-3, AJCA-6, and JCA-9 respectively.

3. RESULTS AND DISCUSSION

3.1. SEM-EDS analysis

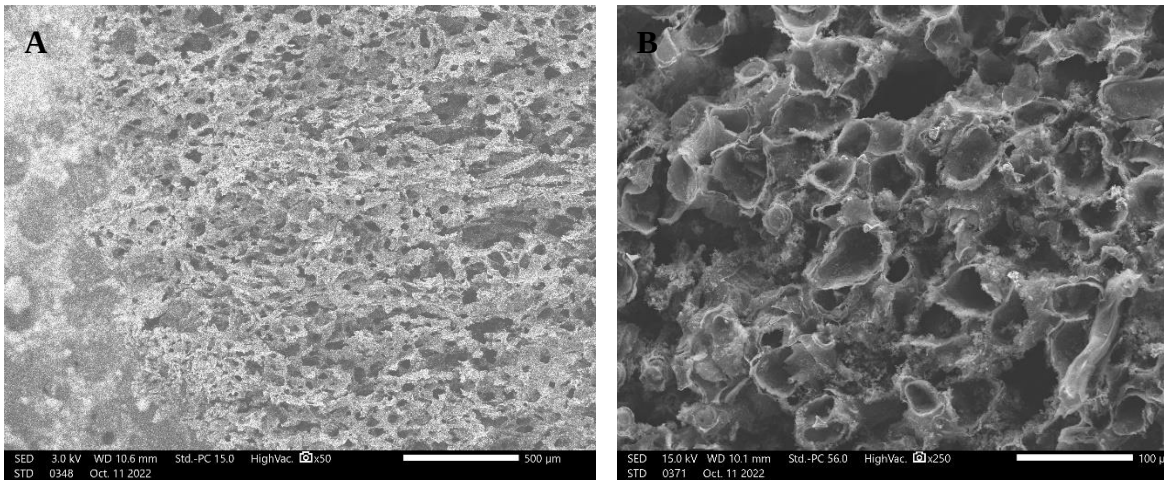

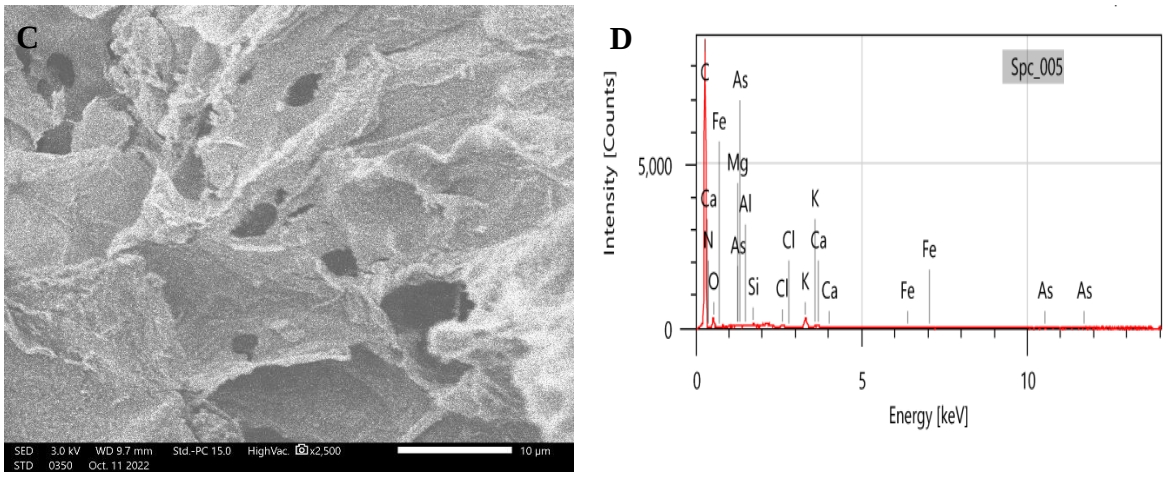

Figure 1. *SEM images of powdered AJCA-3 (A,B,C); EDS elements of powdered AJCA-3 (D).*

The activated carbon aerogel SEM image of AJCA-3 (A, B, C) is shown in figure 1. In figures 1A, B, numerous voids are adjacent to each other with fairly uniform size on the surface of the sample. At 2500 times of the AJCA-3 (figure 1C), the sample surface is quite indented with many holes which is about 2-25 µm in size. It also has a lot of grooves of varying depth, and many layers of scales stack on top of each other.

According to EDS (figure 1D), sample AJCA-3 consists of Carbon 83.77% mass, Oxygen 9.86% mass, Potassium 3.10% mass and other elements. This proves that through the activation process, Oxygen and Potassium adhered to the surface of the airgel sample, expanding the voids in number and size, helping to enhance the adsorption capacity.

3.2. BET analysis

Adsorption-desorption isotherm of N_2 for sample, Fig. 2a, followed a type II isotherm. The amount of specific active surface for AJCA-3 sample according to the analysis represented in Fig. 2b, was 592.65 m^2/g. The correlation coefficient R^2 of BET plot reached 0.99. Furthermore, the pore diameter sizes of AJCA-3 was in the ranges of 2-50 nm (according to IUPAC standards), indicating that it had a mesoporous structure. Additionally, the relative pressure in the range of (P/P_0 = 0 – 0.5) indicates the presence of the material's mesoporous structure. BJH plot illustrated in Fig. 2c shows an average pore diameter at 5.6964 nm.

3.3. Adsorption study

The adsorption equilibrium tests for aerogel carbon materials have been operated with different heating rates (Fig. 4). The adsorption capacity of the materials both increased rapidly in the first 20 minutes and slowly grew in the next 40 minutes. The adsorption capacity changed insignificantly, from min 60 to min 100, suggesting that 60 min is the equilibrium time for CV adsorption by AJCA. In this experiment, the adsorption process took place quickly in the first 20 minutes because the solution contained many CV molecules and the number of empty adsorption centers of the material was still high, so the adsorption process was fast, leading to a rapid increase in the adsorption capacity. Then the number of adsorption sites decreases and the number of CV molecules in the solution also decrease and the solution concentration gradually reaches equilibrium. The maximum adsorption capacity of AJCA-3 is 128.57 mg/g, higher than that of AJCA-6 and AJCA-9 with values of 103.12 and 97.54 mg/g, respectively, showing the influence of the heating rate of the activation process to the adsorption capacity.

The study of CV adsorption kinetics (C_o = 100 ppm) by AJCA material was performed from the experimental values. The values of K_1, $q_{e\_cal,}$ and the correlation coefficient R^2 is shown in

table 1. The value of R^2 for the relationship between $\ln(q_e - q_t)$ and t is from 0.63 – 0.96. However, the equilibrium adsorption capacity values determined from the first-order kinetics equations are significantly different from the experimental values. Therefore, the apparent pseudo-first-order kinetics equation is less suitable for CV adsorption on carbon aerogel materials. The values of R^2 between t/q_t and t according to pseudo-second-order kinetics are all greater than 0.98. Besides, the equilibrium adsorption capacity values calculated from the 2nd-order kinetics equation are close to the experimental values. Therefore, in this study, the apparent quadratic kinetic model is suitable to describe CV adsorption by carbon aerogel, showing that CV adsorption by AJCA is mostly chemisorption. The pseudo-first and pseudo-second-order kinetics models are shown in figures 4a and b.

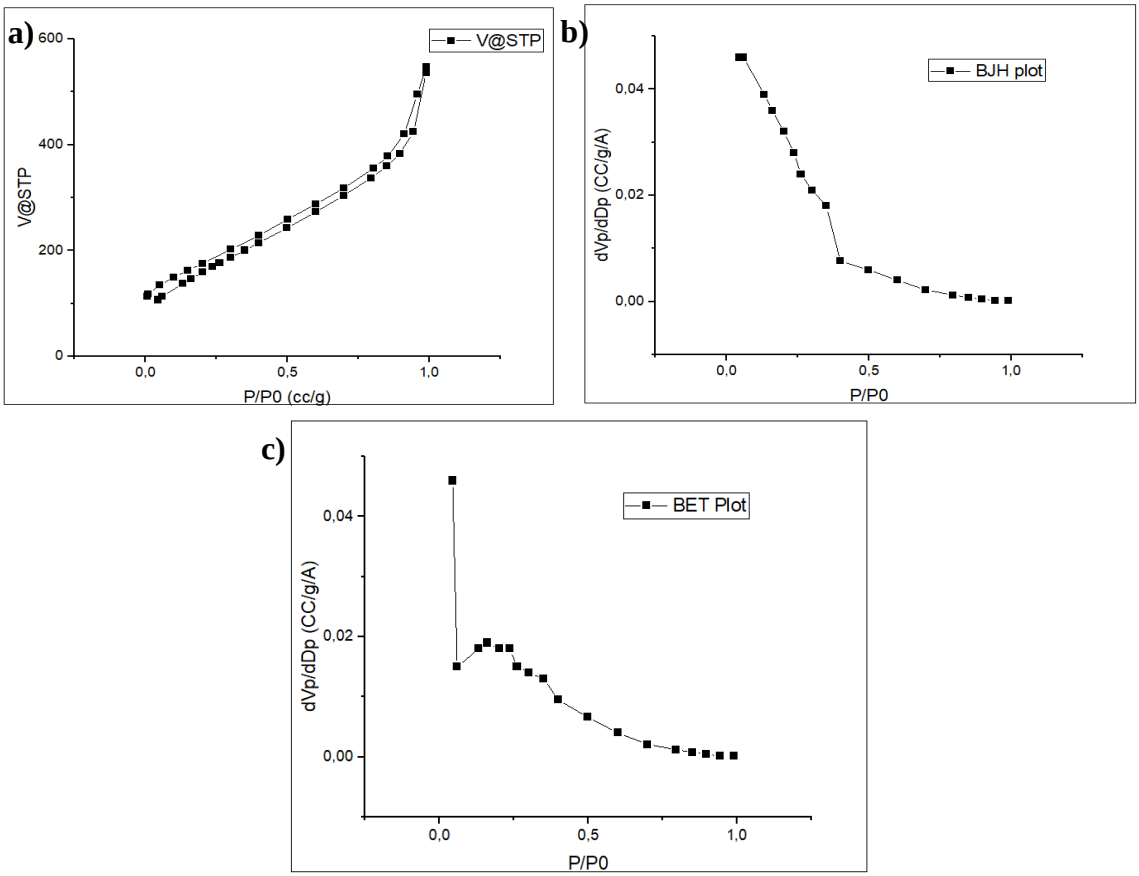

Figure 2. *a) N_2 adsorption - desorption isotherms; b) BET plot and c) BJH plot of AJCA-3.*

The concentration of pollutants is treated as an important design parameter in environmental remediation units. As can be seen in figure 5, as the CV concentration increases from 50 to 300 ppm, the CV adsorption capacity of the material increases gradually. The material with the best adsorption capacity is still AJCA-3, reaching 386.66 mg/g. Figure 3 shows that there is no significant difference between the adsorption capacity of the samples at the concentrations of 50 and 100 ppm. At a concentration of 300 ppm, there is a big difference between AJCA-3 and AJCA-9. The regression analysis of C_e/q_e - Ce in the Langmuir isotherm and $\ln(q_e)$ - $\ln(C_e)$ in the Freundlich isotherm were performed. The isotherm constants were examined correlation coefficients of the Langmuir and Freundlich isotherms are summarized in table 2. It is shown that the correlation coefficient of the Langmuir isotherm is higher (R^2 = 0.9618) than that of the Freundlich isotherm, proving that it is suitable for describing CV adsorption by carbon materials.

The adsorption capacity of materials AJCA-3, AJCA-6, and AJCA-9 at the concentration of 300 ppm tend to approach the q_{max} value calculated from the regression equation of Langmuir isotherm.

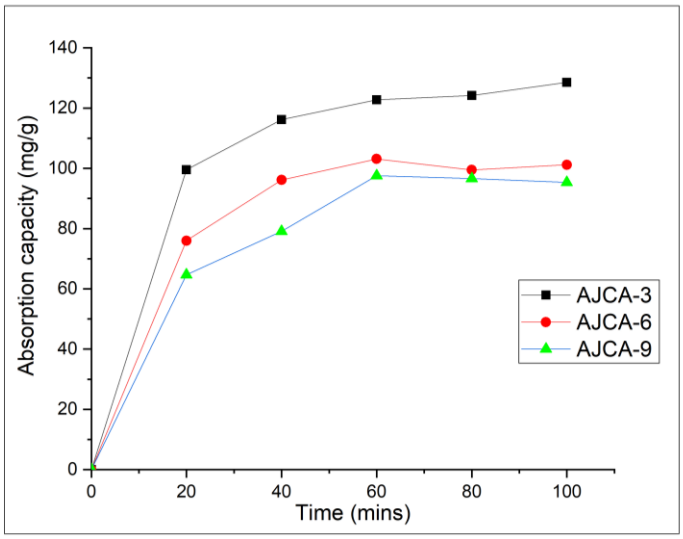

Figure 3. *Adsorption capicity of CV at time.*

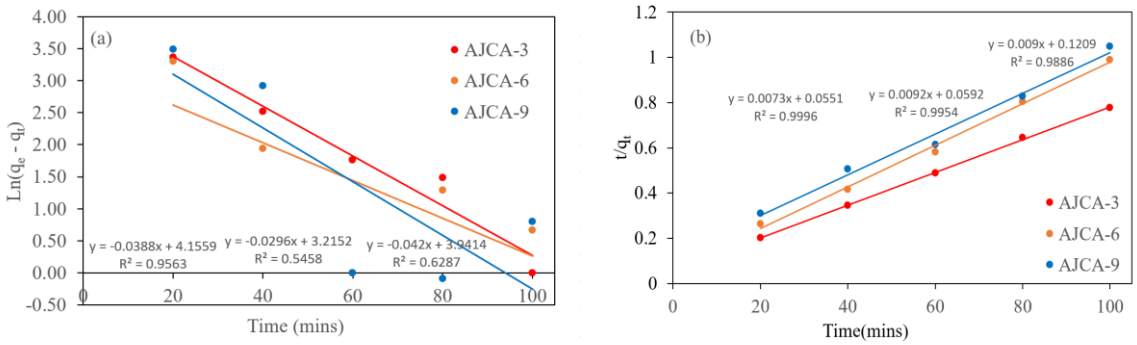

Figure 4. *The pseudo-first and pseudo-second-order kinetics models.*

The effect of pH on the adsorption capacity of AJCA-6 at 300 ppm is shown in Fig. 6. The CV adsorption capacity increased from 311.43 to 379.32 mg/g with increasing pH from 3 to 11 and reached the maximum adsorption capacity. The adsorption capacity of AJCA-6 so unstable that it in this experiment is a little different from it in concentration of solution experiment.

Table 1. *The pseudo-first and pseudo-second-order kinetic parameters of CV adsorption by AJCA.*

	k (min^{-1})	**q_{e_cal} (mg/g)**	**q_{e_exp} (mg/g)**	**R^2**
The pseudo-first order kinetics model				
AJCA-3	0.0388	63.80937	128.57	0.9563
AJCA-6	0.0296	24.90827	103.12	0.5458
AJCA-9	0.042	51.49064	97.54	0.6287
The pseudo-second-order kinetics model				
AJCA-3	0.0009672	136.9863	128.57	0.9996
AJCA-6	0.0014297	108.69565	103.12	0.9954
AJCA-9	0.00067	111.11111	97.54	0.9886

Based on the experimental results of this study, and depending on the structure of the adsorbate and the properties of the adsorbent surface, the mechanism for removing CV by AJCA adsorption may involve the following steps:

(i) Migration of the dye from the solution to the surface of the adsorbent.

(ii) Dye diffusion through the boundary layer on the surface of the adsorbent.

(iii) Adsorption of the dye on the AJCA surface.

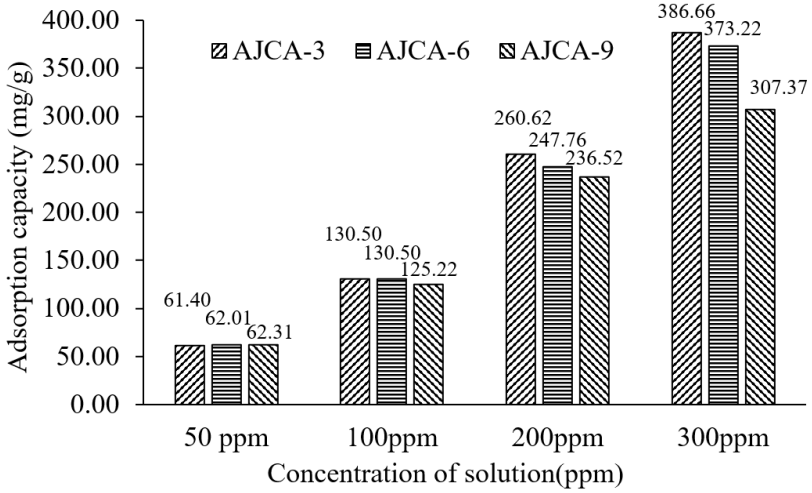

Figure 5. *The CV adsorption capacity of the materials at different concentration of solution.*

Table 2. *The isotherm constants of the Langmuir and Freundlich isotherms.*

	Langmuir			Freundlich		
	q_{max}	q_{exp}	R^2	K_f	n	R^2
AJCA-3	384,62	386,66	0,9618	91,47	1,61	0,8458
AJCA-6	370,37	373,22	0,9729	90,92	2,30	0,8469
AJCA-9	322,58	307,37	0,9883	70,24	2,75	0,9705

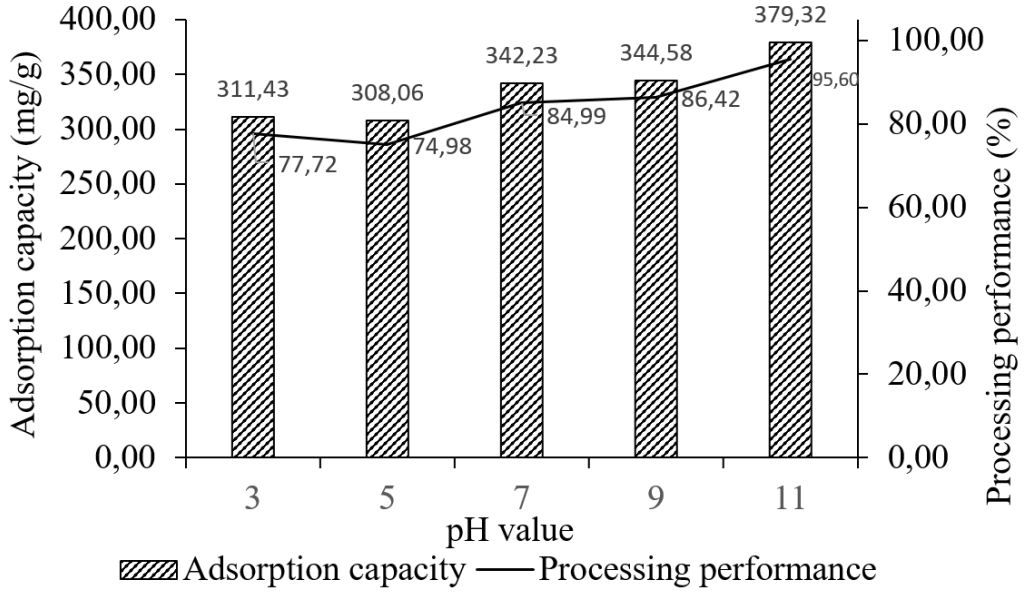

Figure 6. *The effect of pH on the adsorption capacity of AJCA-6.*

Table 3. *Comparison of CV sorption capacity of AJCA-3 with other reported low-cost adsorbents.*

Sorbent	q_{max} (mg/g)	Reference
Activated carbon	420.068 mg/g	[23]
Orange peel	14.3 mg/g	[24]
Skin almond waste	85.47 mg/g	[25]
Treated coir pith	94.7 mg/g	[26]
Chitin-psyllium based aerogel	227.11 mg/g	[27]
Sugarcane bagasse–bentonite/sodium alginate	839.9 mg/g	[28]
Silane-modified cellulose nanofiber aerogel	150 mg/g	[29]
Three-dimensional graphene aerogel	280.8 mg/g	[30]
KOH-activated carbon aerogel	379 mg/g	This study

4. CONCLUSIONS

In this work, an aerogel was synthesized using biowaste as the core of jackfruit. The aerogel developed was used to evaluate its ability to adsorb molecules of crystal violet dye present in aqueous solutions. The aerogel's characterization demonstrated a randomly interconnected hole with a channel structure that resembles an open pore network. These characteristics contribute to the adsorption of dye molecules and may be a consequence of the uncontrolled growth of carbonization. The adsorption was dependent on the contaminant dosage and at 100 ppm, and 300 ppm CV, AJCA-3 respectively removed 100%, and 96% of CV dye from the aqueous solution. The increase in pH caused a significant increase in dye removal percentage, increasing 10,8% in pH = 11. Because of cost benefits, the pH of the CV solution (pH = 7) was considered more suitable for adsorption. The pseudo-second-order model well represented the adsorption kinetics and the Langmuir model was suitable to represent the equilibrium data. The maximum adsorption capacity achieved was 379 $mg.g^{-1}$, which indicates that aerogel is very efficient and competitive with several adsorbents in removing CV from aqueous solutions. In the next study, a regeneration experiment will be conducted to evaluate the reusability of AJCA to remove CV from an aqueous solution. In conclusion, the tests using aerogel to remove the color from a simulated effluent containing different dyes and compounds indicate that aerogel has a high potential to treat real colored effluents.

Acknowledgment: *We acknowledge the contributions of all the reviewers and thank them for their insightful comments on the early drafts of this article. The comments also provide guidance to our studies.*

REFERENCES

[1]. T.C.A. Siqueira, L.Z. da Silva, A.J. Rubio, R. Bergamasco, F. Gasparotto, EAd-S Paccola, et al. *"Sugarcane bagasse as an efficient biosorbent for methylene blue removal: kinetics, isotherms and thermodynamics"*, Int J Environ Res Publ Health, 17, p. 526, (2020).

[2]. S. Noreen, M. Tahira, M. Ghamkhar, I. Hafiz, H.N. Bhatti, R. Nadeem, et al. *"Treatment of textile wastewater containing acid dye using novel polymeric graphene oxide nanocomposites (GO/PAN,GO/PPy, GO/PSty)"*, J Mater Res Technol, 14, pp. 25-35, (2021).

[3]. Organization for Economic Co-operation and Development, Eco-Innovation in Industry, Enabling Green Growth, OECD Innovation Strategy, OECD, Paris, (2009).

[4]. P. Grassi, F.C. Drumm, S.S. Spannemberg, J. Georgin, D. Tonato, M.A. Mazutti, et al. *"Solid wastes from the enzyme production as a potential biosorbent to treat colored effluents containing crystal violet dye"*, Environ Sci Pollut Res, 27, pp. 10484-10494, (2020).

[5]. H. Ali, S.K. Muhammad, *"Biosorption of crystal violet from the water on leaf biomass of Calotropis procera"*, Environ Sci Technol 1, 143–150, (2008).

[6]. R.F. Wang, L.G. Deng, K. Li, X.J. Fan, W. Li, H.Q. Lu, *"Fabrication and characterization of sugarcane bagasse–calcium carbonate composite for the efficient removal of crystal violet dye from wastewater"*, Ceram Int, 46, pp. 27484-27492, (2020).
[7]. V. Buscio, V. López-Grimau, M.D. Álvarez, C. Gutiérrez-Bouzán, *"Reducing the environmental impact of textile industry by reusing residual salts and water: ECUVal system"*, ChemEng J 373, 161–170, (2019).
[8]. C.R. Holkar, A.J. Jadhav, D.V. Pinjari, N.M. Mahamuni, A.B. Pandit, *"A critical review on textile wastewater treatments: possible approaches"*, J. Environ. Manag. 182, 351–366, (2016).
[9]. Z. Jia, Z. Li, T. Ni, S. Li, *"Adsorption of low-cost adsorption materials based on biomass (Cortaderia selloana flower spikes) for dye removal: kinetics, isotherms and thermodynamic studies"*, J Mol Liq, 229, pp. 285-292, (2017).
[10]. K. Lee, L. Shabnam, S.N. Faisal, V.C. Hoang, V.G. Gomes, *"Aerogel from fruit biowaste produces ultracapacitors with high energy density and stability"*, Journal of Energy Storage 27, 101152, (2020).
[11]. Maji, Subrata, et al. *"High-Performance Supercapacitor Materials Based on Hierarchically Porous Carbons Derived from Artocarpus heterophyllus Seed"*. ACS Applied Energy Materials, 4(11), 12257-12266, (2021).
[12]. DAT, Nguyen Tien, et al. *"Carbon sequestration through hydrothermal carbonization of expired fresh milk and its application in supercapacitor"*. Biomass and Bioenergy, 143: 105836, (2020).
[13]. Dabrowski, A., *"Adsorption - from theory to practice"*. Advances in Colloid and Interface Science, 93: p. 135-224, (2001).
[14]. Othman, N.H., et al., *"Adsorption kinetics of methylene blue dyes onto magnetic graphene oxide"*. Journal of Environmental Chemical Engineering, 6(2): p. 2803-2811, (2018).
[15]. Gupta, N., A.K. Kushwaha, and M.C. Chattopadhyaya, *"Application of potato (Solanum tuberosum) plant wastes for the removal of methylene blue and malachite green dye from aqueous solution"*. Arabian Journal of Chemistry, 9: p. S707-S716, (2016).
[16]. Akar, E., A. Altinişik, and Y. Seki, *"Using of activated carbon produced from spent tea leaves for the removal of malachite green from aqueous solution"*. Ecological Engineering, 52, p. 19-27, (2013).
[17]. Qiu, H., et al., *"Critical review in adsorption kinetic models"*. Journal of Zhejiang University-SCIENCE A, 10(5), p. 716-724, (2009).
[18]. K. Vasanth KumarV, R., Sivanesan, *"Biosorption of malachite green, a cationic dye onto Pithophora sp., a fresh water algae"*. Dyes and Pigments, 69, p. 102-107, (2006).
[19]. Largitte, L. and R. Pasquier, *"A review of the kinetics adsorption models and their application to the adsorption of lead by an activated carbon"*. Chemical Engineering Research and Design. 109, p. 495-504, (2016).
[20]. Qiu, H., et al., *"Critical review in adsorption kinetic models"*. Journal of Zhejiang University-science a. 10(5), p. 716-724, (2009).
[21]. Y. S. Ho, G.M., *"The kinetics of sorption of divalent metal ions onto sphagnum moss peat"*. Water Research. 34(3), p. 735-742, (2000).
[22]. C. Hessel, C. Allegre, M. Maisseu, F. Charbit, P. Moulin, *"Guidelines and legislation for dye house effluents"*, J. Environ. Manag. 83 (2), 171–180, (2007).
[23]. Qingsong Ji, Haichao Li, *"High surface area activated carbon derived from chitin for efficient adsorption of Crystal Violet"*, Diamond and Related Materials, 118, 108516, (2021).
[24]. Annadurai, G., Juang, R.-S., & Lee, D.-J. *"Use of cellulose-based wastes for adsorption of dyes from aqueous solutions"*. Journal of Hazardous Materials, 92, 263–274, (2004).
[25]. Atmani, F., Bensmaili, A., & Mezenner, N. Y. *"Synthetic textile effluent removal by skin almond waste"*. Journal of Environmental Science and Technology, 2, 153–169, (2009).
[26]. Chowdhury, S., Mishra, R., Saha, P., & Kushwaha, P. *"Adsorption thermodynamics, kinetics and isosteric heat of adsorption of malachite green onto chemically modified rice husk"*. Desalination, 265, 159–168, (2011).
[27]. Druzian, Susanne P., et al. *"Chitin-psyllium based aerogel for the efficient removal of crystal violet from aqueous solutions"*. International Journal of Biological Macromolecules, 179, 366-376, (2021).
[28]. Gong, Xiao-Li, et al. *"Effective adsorption of crystal violet dye on sugarcane bagasse–bentonite/sodium alginate composite aerogel: Characterisation, experiments, and advanced modelling."* Separation and Purification Technology, 286, 120478, (2022).

[29]. Gopakumar, Deepu A., et al. *"Robust superhydrophobic cellulose nanofiber aerogel for multifunctional environmental applications."* Polymers 11.3, 495, (2019).
[30]. Liu, Cuiyun, et al. *"In situ reduced and assembled three-dimensional graphene aerogel for efficient dye removal."* Journal of Alloys and Compounds 714: 522-529, (2017).

TÓM TẮT

Tổng hợp carbon aerogel hoạt hóa bằng KOH để loại bỏ thuốc nhuộm Crystal violet hiệu quả ra khỏi nước

Trong nghiên cứu này, một sản phẩm carbon aerogel hoạt hóa bằng KOH (AJCA) từ mít được điều chế bằng quá trình xử lý thủy nhiệt lõi của mít với tốc độ gia nhiệt khác nhau. AJCA được tổng hợp để hấp thụ thuốc nhuộm màu tím pha lê Crystal violet (CV) từ dung dịch nước và xử lý hiệu quả các loại thuốc nhuộm khác. Kính hiển vi điện tử quét (SEM) và quang phổ tia X phân tán năng lượng (EDS) cho thấy bề mặt mẫu có nhiều rãnh có độ sâu khác nhau và nhiều lớp vảy xếp chồng lên nhau.. Diện tích bề mặt riêng được kiểm tra bằng phương pháp The Brunauer-Emmett-Teller (BET), đạt 592,65 m^2/g. Tốc độ gia nhiệt phù hợp nhất là 3 độ mỗi phút (AJCA-3). Khả năng hấp phụ tối đa là 386,66 mg/g và hiệu suất hấp thụ đạt 96,5% ở nồng độ 300 ppm, điều này cho thấy AJCA-3 rất hiệu quả và có khả năng cạnh tranh với một số chất hấp phụ. Mô hình bậc hai giả mô tả thỏa đáng động học hấp phụ, và mô hình Langmuir thích hợp để biểu diễn cân bằng hấp phụ. Những thí nghiệm này cho thấy rằng AJCA có tiềm năng tuyệt vời trong việc xử lý các chất sinh màu thực.

Từ khoá: Activated carbon aerogel; Hiệu quả; Crystal violet.